



Machine learning-based model for fatigue behavior analysis of plasma nitrided AISI 304 steel

Erfan Maleki^{a,*}, Okan Unal^{b,c}

a Department of Mechanical Engineering, Politecnico di Milano, Milan, Italy

b Department of Mechanical Engineering, Karabuk University, Karabuk, Turkey

c Modern Surface Engineering Laboratory (MSELAB), Karabuk University, Karabuk, Turkey

P A P E R I N F O

Paper history:

Received 21 July 2023

Received in revised form 29 July 2023

Accepted 29 July 2023

Keywords:

Plasma nitriding; Fatigue; Machine learning; Deep learning; Austenitic stainless steel

A B S T R A C T

Surface treatments play critical role in fatigue behavior improvement of metals. In this study, a machine learning-based model was employed to analyze the effects of plasma nitriding as a thermal surface treatment on improving the fatigue behavior of AISI 304 steel. Experimental data, encompassing various plasma nitriding and fatigue loading conditions, were utilized to train different types of artificial neural networks including shallow neural networks and deep neural networks. The inputs to the model were the process parameters of plasma nitriding, including time and temperature, along with the stress amplitude in the fatigue test. The output parameter was the fatigue life. The findings demonstrated that employing deep neural networks led to higher accuracy in the predictions. Furthermore, the obtained results of conducted parametric analyses indicated that the optimal temperature range for achieving the highest fatigue performance lies between approximately 450-550 °C for more than 4 h.

1. INTRODUCTION

AISI 304, an austenitic stainless steel, has become widely favored in various applications because of its excellent corrosion resistance, nonmagnetic properties, and biocompatible characteristics. Nevertheless, it lacks sufficient hardness, strength, and wear resistance, prompting the need for further enhancements by applying post-treatments [1,2]. Consequently, both mechanical surface treatments, such as surface mechanical attrition treatment (SMAT) [3], shot peening (SP) [4], and ultrasonic nanocrystal surface modification (UNSM) [5], as well as thermal surface treatments like carburizing [6] and plasma nitriding (PN) [7], have been employed to enhance hardness and wear and corrosion resistance as well as considerable fatigue behavior improvement.

Dealing with PN process, to achieve a sufficient wear resistance/fatigue performance, the application of nitriding processes is crucial, leading to the creation of thick nitride layers on the top surface. This improvement can be attributed to the unique characteristics of the nitrided zone. The thickness of the nitrided layer varies depending on the type of process, operating temperature, duration, and chamber environment. Nonetheless, high processing temperatures and

prolonged durations tend to cause distortion in metal parts, which is generally undesirable. To mitigate this issue, PN,

performed under high-density plasma with low vacuum pressure, proves advantageous, as it allows for reduced temperature and duration without compromising the performance of the nitrided surfaces [8,9]. This treatment has been further refined through the implementation of glow discharge, which involves adjusting voltage and current. Glow discharge enables ionization, and the ions are then bombarded onto surfaces through a high voltage difference [10,11]. By exposing thermally treated surfaces to plasma energy, the outcomes are significantly improved in a shorter time and at lower temperatures, as diffusion is accelerated, resulting in a controllable microstructure formation [12–14].

Considering austenitic stainless steels, PN has emerged as a widely chosen method to enhance the surface properties, which is primarily sought after for its corrosion resistance in industrial applications. However, it is essential to maintain a reasonable balance between wear and fatigue resistance. As a result, numerous investigations have been carried out to explore various surface treatments. PN is a thermo-mechanical process applied within a temperature range of 350–550°C. Thanks to the accelerated plasma energy, nitrogen atoms can diffuse more rapidly compared to conventional methods [15,16]. This results in the formation of a body-centered tetragonal expanded austenite (S-phase), leading to a significant increase in the surface hardness of austenitic stainless steels up to about HV 1000 [17,18].

In the case of steels with an austenitic structure, they tend to transform into a metastable supersaturated nitrogen-rich S-

*Corresponding Author Email: maleky.erfan@gamil.com

(Dr. Erfan Maleki)

phase when subjected to temperatures above 450°C. This transformation brings about high hardness and improved wear resistance performance. However, a notable decrease in corrosion resistance occurs due to the onset of CrN precipitation, resulting from a reduction in the chromium content within the matrix. To overcome this issue, Díaz-Guillén et al. [19] demonstrated a method of combining the S-phase with a chromium-nitrided structure through pulsed plasma nitriding carried out in the temperature range of 510–550°C. Another study by Lu et al. [20] revealed that nitriding efficiency is relatively low at 450°C. The primary advantage of the treatment lies in efficiently developing the S-phase without compromising the corrosion resistance performance. As a result, research efforts have been focused on finding ways to rapidly produce the S-phase.

In our previous study [21], the pulsed PN treatment was applied to AISI 304 austenitic stainless steel at various temperatures and durations. This study aimed to establish an exact boundary for microstructural and mechanical behaviors concerning pulsed PN conditions. The results revealed that the nitriding depth increased as the process temperature and duration were enhanced. Particularly remarkable increases in nitriding depth were observed at 475°C for 8 hours and at 550°C for 4 hours. During the low-temperature PN, the austenite structure transformed into a metastable nitrogen-oversaturated body-centered tetragonal expanded austenite (S-phase). Subsequently, the S-phase converted to CrN precipitation at 475°C for 8 hours and at 550°C for 4 hours. Surface hardness and fatigue limit experienced an enhancement through PN, irrespective of the process conditions. The best surface hardness and fatigue limit were obtained at 550°C for 4 hours due to the occurrence of CrN precipitation.

On the other hand, in recent years, machine learning (ML)-based models, particularly artificial neural networks (ANNs), have gained widespread acceptance as a viable solution for addressing complex problems [22–25]. The massively parallel structure of ANNs enables them to handle multivariable nonlinear modeling, where obtaining accurate analytical solutions would otherwise be very challenging [26–28]. These systems possess the ability to learn from examples, demonstrate fault tolerance by handling noisy and incomplete data, effectively deal with nonlinear problems, and exhibit high-speed prediction and generalization capabilities once trained [29,30]. In the realm of ANN applications for modeling the fatigue behavior of materials, significant research has been conducted. A substantial portion of these ANN models is focused on the prediction of fatigue life in different materials [31–38]. In general, an ANN is composed of three major layers: input, hidden, and output. The initial generation of ANNs known as shallow neural networks (SNN), was widely employed for simulating various processes. SNNs typically consist of 1 or 2 hidden layers and are commonly trained using the back-propagation (BP) algorithm. Despite their usefulness, SNNs have certain limitations, with the most significant being the requirement for a large dataset during development [39]. Significant progress has been made in the development of ANNs through deep learning methods, such as the restricted Boltzmann machine (RBM) and deep belief network (DBN) introduced by Hinton et al. in 2006 [40,41]. These advancements have paved the way for the creation of deep

neural networks (DNNs) using a layer-wise pre-training approach, which has proven to be highly effective.

In this study, following our previous experimental study on the application of on PN on AISI 304 [21], ML-based models considering SNN and DNN approaches considered for fatigue behavior prediction and analyses. The experimental data is utilized to train and develop the model. The input parameters considered were stress amplitude, time and temperature of the PN process, while the output parameter of the model was the fatigue life. The performance of the ML-based model was evaluated thoroughly and showed excellent agreement when compared with the experimental results.

2. EXPERIMENTAL PROCEDURE

Firstly, it should be mentioned that entire experimental procedures/data used in this study were achieved from our previous study [21]. AISI 304 austenitic stainless steel samples were produced using cold drawn bars after undergoing quenching and annealing at a temperature of 1050°C. The PN process was carried out in a PLC-controlled pulsed furnace. A gas mixture consisting of 25vol% N₂ and 75vol% H₂ was introduced into the chamber, selected based on the effectiveness of having 15vol%–30vol% of N₂ [42]. The chamber pressure was set at approximately 500 Pa with a potential of 500 V, and the accepted range for pressure was 100–130 Pa [43]. For the novel approaches, the conditions were adjusted to 500 V potential and 333 Pa vacuum pressure [44]. While maintaining common chamber conditions for all nitriding processes, initial parameters were established by referring to previous approaches that examined the impact of nitriding temperature and duration on microstructural and mechanical performance. Each parameter's effect was assessed independently by keeping the temperature and duration constant. The specific plasma nitriding conditions of the specimens were included 400°C for 4 h, 475°C for 2 h, 475°C for 4 h, 475°C for 8 h and 550°C for 4 h. Subsequent fatigue tests were conducted using a BESMAK BMT-250 rotating bending fatigue tester, employing a frequency of 50 Hz and a constant stress amplitude of $R = -1$. Load control was manual with a load cell, and the tests were conducted using the DOLI software.

3. IMPLEMENTATION OF MACHINE LEARNING MODEL

ANNs are inspired by the remarkable capabilities of the human brain in understanding complex problems and offering logical solutions based on functional relationships. These networks are valuable tools for modeling and analyzing intricate and non-linear processes that involve multiple variables. They excel at handling and unraveling non-linear processes influenced by various factors [28].

The methodology employed in this study for implementation of ML-based model is illustrated in Fig. 1a. An iterative trial and error approach was utilized to develop various SNNs and DNNs. Fig. 1b displays the architecture of the DNN with four hidden layers, denoted by w , b , and f , representing the weight matrices, bias vectors, and transfer functions for each respective layer.

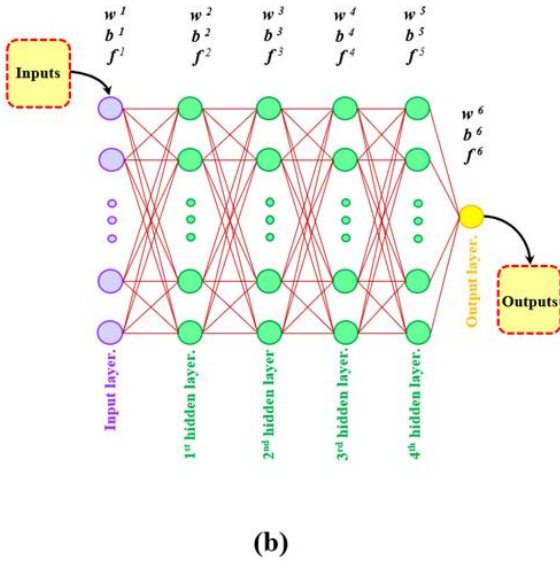
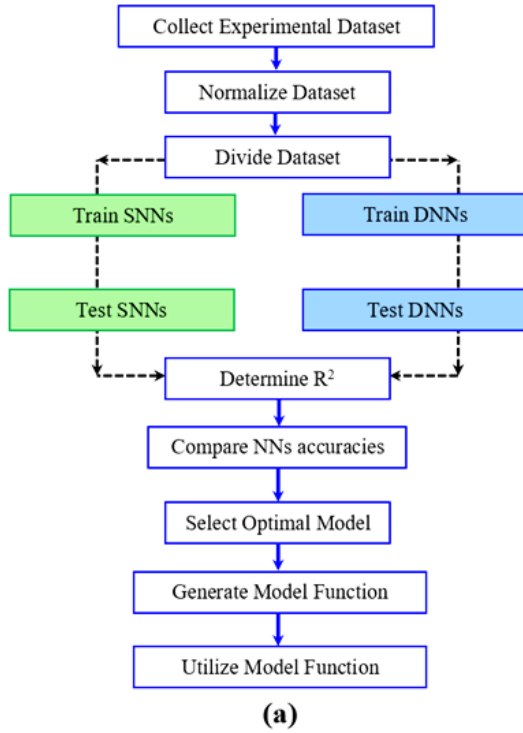


Figure 1. (a) The considered methodology in this study for implementation of ML-based models and (b) schematic illustration of a DNN with 6 layers adopted form [45].

The considered input parameters for the model were the stress amplitude, time and temperature of the PN process, while the output parameter was the fatigue life. The number of neurons serving as computational nodes in the ANNs, plays a crucial role in determining the efficiency of the applied models. The accuracy of the predicted results from these networks, assessed using the correlation coefficient (R^2), served as the measure of

efficiency for each developed network. The R^2 value was calculated as follows:

$$R^2 = \frac{\sum_{i=1}^n (f_{EXP,i} - F_{EXP})(f_{ANN,i} - F_{ANN})}{\sqrt{\sum_{i=1}^n ((f_{EXP,i} - F_{EXP})^2 (f_{ANN,i} - F_{ANN})^2)}} \quad (1)$$

Where 'n' is the number of samples used for training and testing, and ' f_{EXP} ' and ' f_{ANN} ' represent the experimental and predicted values, respectively. The values of F_{EXP} and F_{ANN} are determined by:

$$F_{EXP} = \frac{1}{n} \sum_{i=1}^n f_{EXP,i} \quad (2.a)$$

$$F_{ANN} = \frac{1}{n} \sum_{i=1}^n f_{ANN,i} \quad (2.b)$$

The accuracy of the results for several developed SNNs with 1 and 2 hidden layers, each with different numbers of neurons, was compared to get the optimum network structure. In addition, it should be mentioned that a learning rate of 0.190, and Logarithmic Sigmoid transfer functions were used in all developed models.

4. RESULTS AND DISCUSSION

4.1. Experimental Results

The S-N curves depicting the stress amplitude versus the number of cycles for all treated specimens are presented in Fig. 2a. When subjected to a certain stress amplitude, the S-N curve of iron-based alloys levels off, indicating the potential for infinite life. The fatigue limit of the as-received AISI 304 (PN time=0 h and temperature=20 °C) is measured as 215 MPa. However, after nitriding at 400°C for 4 hours, the fatigue limit increased to 260 MPa. It's important to note that at this temperature and duration, the nitrided layer is too thin to be accurately measured. The observed changes in fatigue limits can be attributed to the high-temperature regime with nitrogen affecting the surface. Through heating and cooling processes, the surface undergoes modification with a hard deposition. Notably, the fatigue limit shows significant improvement, reaching 355 MPa at 475°C for 2 hours and further increasing to 600 MPa at 550°C for 4 hours. Additionally, the endurance limits are close to each other at 475°C for 8 hours and at 550°C for 4 hours. Despite the similar nitrided zone thicknesses at 475°C for different durations, the treatment lasting 8 hours results in an effectively enhanced fatigue resistance (more details can be get in [21]). Fig. 2b reveals the determined fatigue limits for all considered sets.

Fig. 3 illustrates the fatigue fracture surface of both the as-received and treated specimens. In the as-received specimen (see Fig. 3a), failure occurs due to the presence of multiple crack initiation sites supported by inner micro-cracks. However, during short nitriding durations, the surface compression resulting from residual stress and the presence of a hardened zone reduces the surface crack initiation zone, leading to the subsurface inner micro-cracks becoming the primary contributors to fracture (see Fig. 3b-3d). Furthermore, inclusions play a significant role in the fatigue fracture

mechanism. These inclusions create stress concentrations, making them act as the points for initial micro-crack formation.

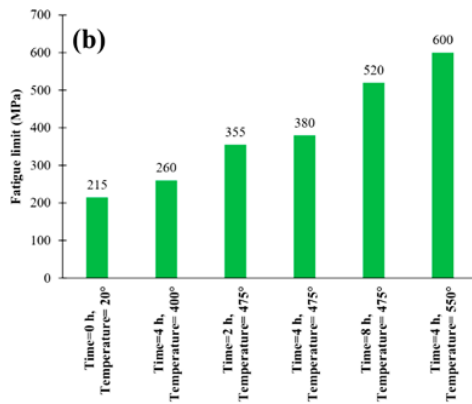
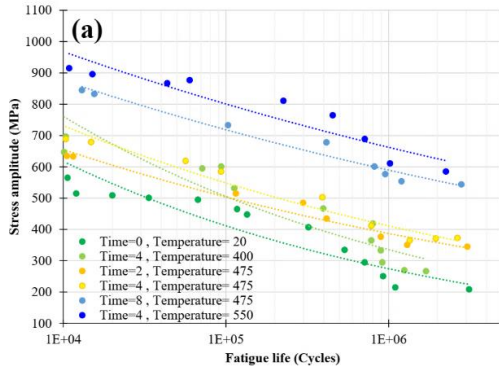
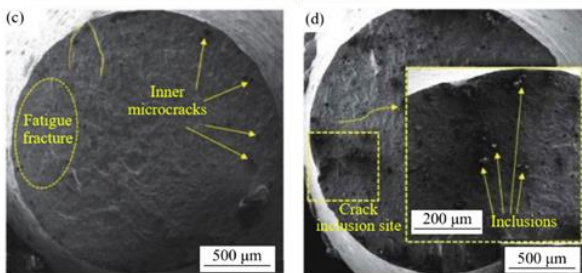


Figure 2. (a) The obtained S-N curves for as-received and plasma nitrided AISI 304 specimens under rotating bending fatigue loads at room temperature and stress ratio of -1;



adopted from [21]. (b) The determined fatigue limits for all considered sets.

Figure 3. SEM observations from fractography of the different sets of (a) as received, (b) nitrided at 400°C for 4 h, (c) nitride at 475°C for 2 h and (d) nitrided at 475°C for 4 h; adopted from [21].

4.2. Modelling Results

Fig. 4a displays the performance of the developed SNNs concerning the number of neurons utilized in each layer. It is evident from the graph that SNNs with a higher number of nodes yield more accurate results compared to others. However, the SNN with the highest efficiency, consisting of 2 hidden layers and 50 neurons in each layer, achieved an accuracy factor of 0.82, which was not considered satisfactory for further analysis. Fig. 4b illustrates the influence of the number of hidden layers on both the considered SNNs and DNNs. Increasing the depth of the network led to enhanced accuracy for the same dataset. Interestingly, when maintaining an equal learning rate of 0.190, a higher accuracy of approximately 0.99 could be achieved by reducing the number of nodes. Through a trial-and-error approach, various NNs were developed, and among them, the DNN with an architecture of 2-40-15-9-6-2 was selected for further analysis. The mentioned network exhibited R2 values of 0.993 and 0.971 for training and testing steps respectively. The obtained accuracy values were found to be highly acceptable, indicating the successful development of the networks. The first layer of the chosen DNN utilized a Tangential sigmoid activation function, while the hidden and output layers employed a logarithmic Sigmoid transfer function.

After successful developing of DNN with remarkable accuracy, the generated model function allows for conducting parametric analyses across the entire range of input parameters. These parametric analyses offer valuable insights into how the output, fatigue life, varies with changes in the input parameters, such as time and temperature of the PN process. The ANNs, being highly efficient in handling complex and nonlinear relationships, enable a comprehensive exploration of the entire parameter space, leading to a deeper understanding of the fatigue behavior of treated AISI 304. The capability to conduct parametric analyses opens up paths for optimizing and fine-tuning the process conditions to achieve desired outcomes. By identifying the optimal set of input parameters, it becomes possible to enhance the mechanical properties and fatigue performance of materials while ensuring efficient utilization of resources and reducing costs.

Fig.5 displays the 2D contours representing the relationship between stress amplitude, temperature of the PN process, and fatigue life. The findings demonstrate that the highest fatigue performance is attainable within the temperature range of approximately 450-550 °C for each corresponding time duration. Furthermore, the results show that increasing the time intervals leads to an enhancement in the efficiency of PN, resulting in improved fatigue behavior. Overall, the observations suggest that the simultaneous

optimization of both the time and temperature of the PN process leads to the best fatigue performance. These findings hold high implications for material engineering and structural design. By identifying the optimal combinations of stress amplitude, temperature, and time of PN, processing conditions to maximize the fatigue life of AISI 304 can be tailored. Such knowledge is essential in enhancing the reliability, durability, and performance of components subjected to cyclic loading, thereby contributing to improved safety and efficiency in various applications. Additionally, the insights gained from the conducted parametric analyses (2D contours) provide a valuable reference for PN process optimization in industries such as aerospace, automotive, and mechanical engineering, where fatigue failure can have severe consequences.

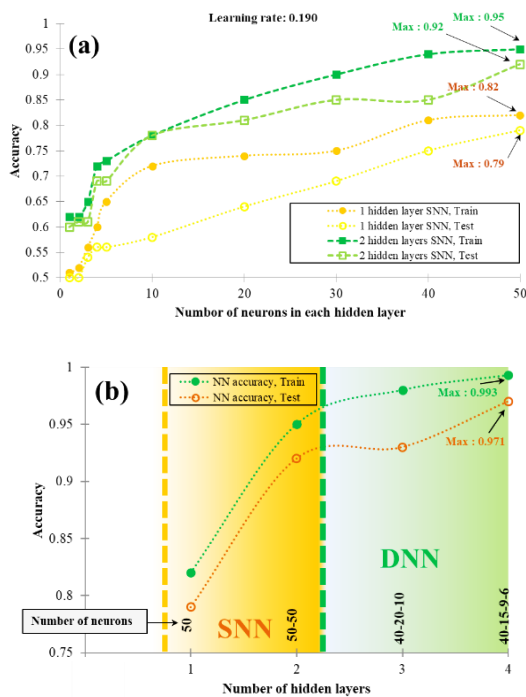


Figure 4. (a) Performance evaluation of the developed SNNs with 1 and 2 hidden layer considering the number of utilized neurons in each layer. (b) Comparison of the accuracy of NNs with different depths of 1, 2, 3 and 4 hidden layers.

5. CONCLUSIONS

In this study, effects of PN on fatigue behavior improvement of AISI 304 were modeled and analyzed through a machine learning-based model. Experimental results considering different conditions of plasma nitriding and fatigue loading were used to feed to the different neural networks. In addition, different types of ANNs including SNNs and DNNs were developed and a network which had the highest performance was selected for further analysis. Process parameters of PN including time and temperature as well as stress amplitude in fatigue test were regarded as inputs and fatigue life was considered as output. Based on the obtained results the following conclusions can be drawn:

- Higher accuracy can be obtained by using deeper DNN compared to SNN. The selected DNN with structure of 2-40-15-9-6-2 exhibited considerable R^2 values of 0.993 and 0.971 for training and testing steps respectively.
- Highest fatigue performance can be achieved within the temperature range of approximately 450-550 °C. Moreover, increasing the time intervals enhances the efficiency of the PN process, leading to improved fatigue behavior.
- By efficiently modeling and predicting outcomes based on complex input data, these advanced DNNs have the potential to revolutionize the way we approach problem-solving and decision-making processes. The combination of accurate DNNs and in-depth parametric analyses empowers researchers and practitioners to make data-driven decisions, leading to improved performance, reliability, and cost-effectiveness in a wide range of applications.

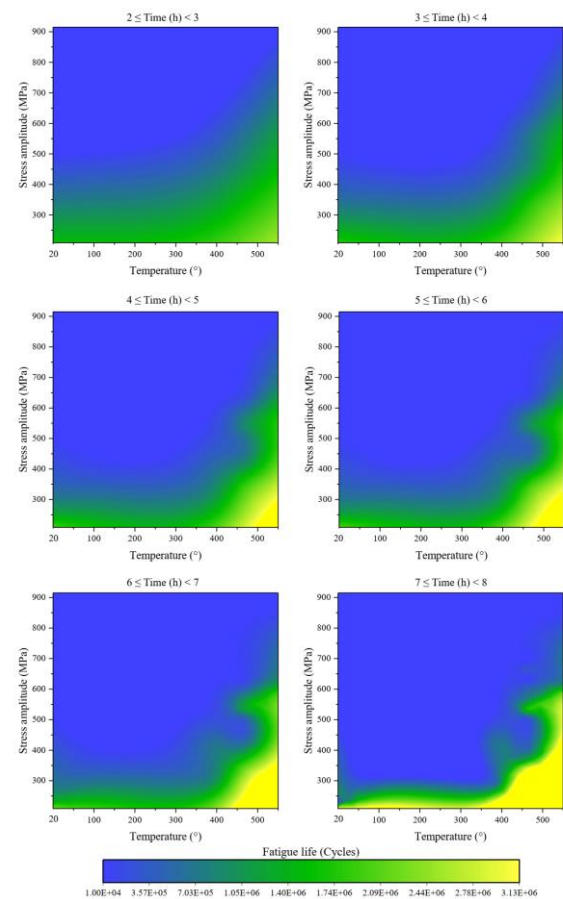


Figure 5. Parametric analysis results in terms of 2D contours of stress amplitude and PN temperature versus fatigue life of AISI 304 obtained by DNN.

ACKNOWLEDGEMENT

The authors would like to extend their sincere gratitude to Prof. G. H. Farrahi for his pivotal role in founding the Journal

of Design Against Fatigue (JDAF). By introducing this innovative and visionary approach, along with a comprehensive scope in the field of fatigue failure, the journal holds the promise of addressing crucial knowledge gaps.

CONFLICTS OF INTEREST

The authors declare that they have no known competing financial interests or personal relationships that could have appeared to influence the work reported in this paper.

REFERENCES

- O. Unal, R. Varol, Surface severe plastic deformation of AISI 304 via conventional shot peening, severe shot peening and re-peening, *Appl. Surf. Sci.* 351 (2015) 289–295. <https://doi.org/10.1016/j.apsusc.2015.05.093.b>
- E. Maleki, O. Unal, Fatigue limit prediction and analysis of nano-structured AISI 304 steel by severe shot peening via ANN, *Eng. Comput.* 37 (2021) 2663–2678. <https://doi.org/10.1007/s00366-020-00964-6>.
- S. Liu, S.Y. Gao, Y.F. Zhou, X.L. Xing, X.R. Hou, Y.L. Yang, Q.X. Yang, A research on the microstructure evolution of austenite stainless steel by surface mechanical attrition treatment, *Mater. Sci. Eng. A.* 617 (2014) 127–138. <https://doi.org/10.1016/j.msea.2014.08.049>.
- A. Tevlek, H.M. Aydın, E. Maleki, R. Varol, O. Unal, Effects of severe plastic deformation on pre-osteoblast cell behavior and proliferation on AISI 304 and Ti-6Al-4V metallic substrates, *Surf. Coatings Technol.* 366 (2019) 204–213. <https://doi.org/10.1016/j.surfcoat.2019.03.034>.
- A. Amanov, R. Karimbaev, E. Maleki, O. Unal, Y.S. Pyun, T. Amanov, Effect of combined shot peening and ultrasonic nanocrystal surface modification processes on the fatigue performance of AISI 304, *Surf. Coatings Technol.* 358 (2019) 695–705. <https://doi.org/10.1016/j.surfcoat.2018.11.100>.
- L. Ceschini, C. Chiavari, E. Lanzoni, C. Martini, Low-temperature carburised AISI 316L austenitic stainless steel: Wear and corrosion behaviour, *Mater. Des.* (2012). <https://doi.org/10.1016/j.matdes.2012.02.019>.
- O. Unal, E. Maleki, R. Varol, Plasma nitriding of gradient structured AISI 304 at low temperature: Shot peening as a catalyst treatment, *Vacuum.* 164 (2019) 194–197. <https://doi.org/10.1016/j.vacuum.2019.03.027>.
- H. Ferkel, M. Glatzer, Y. Estrin, R.Z. Valiev, C. Blawert, B.L. Mordike, RF plasma nitriding of severely deformed iron-based alloys, *Mater. Sci. Eng. A.* (2003). [https://doi.org/10.1016/S0921-5093\(02\)00687-1](https://doi.org/10.1016/S0921-5093(02)00687-1).
- E. Maleki, S. Bagherifard, M. Bandini, M. Guagliano, Surface post-treatments for metal additive manufacturing: Progress, challenges, and opportunities, *Addit. Manuf.* 37 (2021) 101619. <https://doi.org/10.1016/j.addma.2020.101619>.
- K. Nikolov, K. Bunk, A. Jung, P. Kaestner, G. Bräuer, C.P. Klages, High-efficient surface modification of thin austenitic stainless steel sheets applying short-time plasma nitriding by means of strip hollow cathode method for plasma thermochemical treatment, *Vacuum.* (2014). <https://doi.org/10.1016/j.vacuum.2014.09.002>.
- O. Unal, E. Maleki, R. Varol, Effect of severe shot peening and ultra-low temperature plasma nitriding on Ti-6Al-4V alloy, *Vacuum.* 150 (2018) 69–78. <https://doi.org/10.1016/j.vacuum.2018.01.027>.
- S. Corujeira Gallo, H. Dong, On the fundamental mechanisms of active screen plasma nitriding, *Vacuum.* (2009). <https://doi.org/10.1016/j.vacuum.2009.07.002>.
- H. Aghajani, M. Torshizi, M. Soltanich, A new model for growth mechanism of nitride layers in plasma nitriding of AISI H11 hot work tool steel, *Vacuum.* (2017). <https://doi.org/10.1016/j.vacuum.2017.03.032>.
- M. Ozturk, F. Husem, I. Karademir, E. Maleki, A. Amanov, O. Unal, Fatigue crack growth rate of AISI 4140 low alloy steel treated via shot peening and plasma nitriding, *Vacuum.* 207 (2023) 111552. <https://doi.org/10.1016/j.vacuum.2022.111552>.
- R. Kertscher, S.F. Brunatto, On the kinetics of nitride and diffusion layer growth in niobium plasma nitriding, *Surf. Coatings Technol.* (2020). <https://doi.org/10.1016/j.surfcoat.2020.126220>.
- J. Fernández de Ara, E. Almandoz, J.F. Palacio, G.G. Fuentes, Simultaneous ageing and plasma nitriding of grade 300 maraging steel: How working pressure determines the effective nitrogen diffusion into narrow cavities, *Surf. Coatings Technol.* (2017). <https://doi.org/10.1016/j.surfcoat.2017.02.060>.
- L. Shen, L. Wang, Y. Wang, C. Wang, Plasma nitriding of AISI 304 austenitic stainless steel with pre-shot peening, *Surf. Coatings Technol.* (2010). <https://doi.org/10.1016/j.surfcoat.2010.03.018>.
- R. Valencia-Alvarado, A. de la Piedad-Beneitez, J. de la Rosa-Vázquez, R. López-Callejas, S.R. Barocio, O.G. Godoy-Cabrera, A. Mercado-Cabrera, R. Peña-Eguiluz, A.E. Muñoz-Castro, Nitriding of AISI 304 stainless steel in a 85% H₂/15% N₂ mixture with an inductively coupled plasma source, *Vacuum.* (2008). <https://doi.org/10.1016/j.vacuum.2008.03.087>.
- J.C. Díaz-Guillén, M. Naeem, J.L. Acevedo-Dávila, H.M. Hdz-García, J. Iqbal, M.A. Khan, J. Mayen, Improved Mechanical Properties, Wear and Corrosion Resistance of 316L Steel by Homogeneous Chromium Nitride Layer Synthesis Using Plasma Nitriding, *J. Mater. Eng. Perform.* (2020). <https://doi.org/10.1007/s11665-020-04653-9>.
- S. Lu, X. Zhao, S. Wang, J. Li, W. Wei, J. Hu, Performance enhancement by plasma nitriding at low gas pressure for 304 austenitic stainless steel, *Vacuum.* (2017). <https://doi.org/10.1016/j.vacuum.2017.09.020>.
- O. Unal, E. Maleki, R. Varol, Comprehensive analysis of pulsed plasma nitriding preconditions on

- the fatigue behavior of AISI 304 austenitic stainless steel, *Int. J. Miner. Metall. Mater.* (2021). <https://doi.org/10.1007/s12613-020-2097-x>.
22. K. Reza Kashyzadeh, E. Maleki, Experimental Investigation and Artificial Neural Network Modeling of Warm Galvanization and Hardened Chromium Coatings Thickness Effects on Fatigue Life of AISI 1045 Carbon Steel, *J. Fail. Anal. Prev.* 17 (2017) 1276–1287. <https://doi.org/10.1007/s11668-017-0362-8>.
 23. M. Jahanshahi, E. Maleki, A. Ghiami, On the efficiency of artificial neural networks for plastic analysis of planar frames in comparison with genetic algorithms and ant colony systems, *Neural Comput. Appl.* 28 (2017) 3209–3227. <https://doi.org/10.1007/s00521-016-2228-5>.
 24. E. Maleki, Modeling of Severe Shot Peening Effects to Obtain Nanocrystalline Surface on Cast Iron Using Artificial Neural Network, in: *Mater. Today Proc.*, 2016: pp. 2197–2206. <https://doi.org/10.1016/j.matpr.2016.04.126>.
 25. E. Maleki, O. Unal, Shot Peening Process Effects on Metallurgical and Mechanical Properties of 316 L Steel via: Experimental and Neural Network Modeling, *Met. Mater. Int.* 27 (2021) 262–276. <https://doi.org/10.1007/s12540-019-00448-3>.
 26. E. Maleki, G.H. Farrahi, Modelling of conventional and severe shot peening influence on properties of high carbon steel via artificial neural network, *Int. J. Eng. Trans. B Appl.* 31 (2018) 382–393. <https://doi.org/10.5829/jje.2017.30.11b.00>.
 27. E. Maleki, G.H. Farrahi, K. Sherafatnia, Application of artificial neural network to predict the effects of severe shot peening on properties of low carbon steel, 2016. https://doi.org/10.1007/978-981-10-1082-8_5.
 28. N. Maleki, S. Kashanian, E. Maleki, M. Nazari, A novel enzyme based biosensor for catechol detection in water samples using artificial neural network, *Biochem. Eng. J.* 128 (2017) 1–11. <https://doi.org/10.1016/j.bej.2017.09.005>.
 29. E. Maleki, M.J. Mirzaali, M. Guagliano, S. Bagherifard, Analyzing the mechano-bactericidal effect of nano-patterned surfaces on different bacteria species, *Surf. Coatings Technol.* 408 (2021). <https://doi.org/10.1016/j.surfcoat.2020.126782>.
 30. E. Maleki, S. Bagherifard, M. Guagliano, Application of artificial intelligence to optimize the process parameters effects on tensile properties of Ti-6Al-4V fabricated by laser powder-bed fusion, *Int. J. Mech. Mater. Des.* 18 (2022) 199–222. <https://doi.org/10.1007/s10999-021-09570-w>.
 31. K.L. Xiang, P.Y. Xiang, Y.P. Wu, Prediction of the fatigue life of natural rubber composites by artificial neural network approaches, *Mater. Des.* (2014). <https://doi.org/10.1016/j.matdes.2013.12.044>.
 32. E. Maleki, O. Unal, M. Guagliano, S. Bagherifard, Analysing the Fatigue Behaviour and Residual Stress Relaxation of Gradient Nano-Structured 316L Steel Subjected to the Shot Peening via Deep Learning Approach, *Met. Mater. Int.* 28 (2022) 112–131. <https://doi.org/10.1007/s12540-021-00995-8>.
 33. J.Y. Kang, B.I. Choi, H.J. Lee, J.S. Kim, K.J. Kim, Neural network application in fatigue damage analysis under multiaxial random loadings, *Int. J. Fatigue.* (2006). <https://doi.org/10.1016/j.ijfatigue.2005.04.012>.
 34. T. Shi, J. Sun, J. Li, G. Qian, Y. Hong, Machine learning based very-high-cycle fatigue life prediction of AISi10Mg alloy fabricated by selective laser melting, *Int. J. Fatigue.* (2023). <https://doi.org/10.1016/j.ijfatigue.2023.107585>.
 35. M. Bartošák, Using machine learning to predict lifetime under isothermal low-cycle fatigue and thermo-mechanical fatigue loading, *Int. J. Fatigue.* (2022). <https://doi.org/10.1016/j.ijfatigue.2022.107067>.
 36. E. Maleki, S. Bagherifard, S.M.J. Razavi, M. Bandini, A. du Plessis, F. Berto, M. Guagliano, On the efficiency of machine learning for fatigue assessment of post-processed additively manufactured AISi10Mg, *Int. J. Fatigue.* 160 (2022) 106841. <https://doi.org/10.1016/j.ijfatigue.2022.106841>.
 37. J. Horňas, J. Běhal, P. Homola, S. Senck, M. Holzleitner, N. Godja, Z. Pásztor, B. Hegedüs, R. Doubava, R. Růžek, L. Petrusová, Modelling fatigue life prediction of additively manufactured Ti-6Al-4V samples using machine learning approach, *Int. J. Fatigue.* (2023). <https://doi.org/10.1016/j.ijfatigue.2022.107483>.
 38. Z. Zhan, H. Li, Machine learning based fatigue life prediction with effects of additive manufacturing process parameters for printed SS 316L, *Int. J. Fatigue.* 142 (2021). <https://doi.org/10.1016/j.ijfatigue.2020.105941>.
 39. E. Maleki, O. Unal, S.M. Seyedi Sahebari, K. Reza Kashyzadeh, I. Danilov, Application of Deep Neural Network to Predict the High-Cycle Fatigue Life of AISI 1045 Steel Coated by Industrial Coatings, *J. Mar. Sci. Eng.* (2022). <https://doi.org/10.3390/jmse10020128>.
 40. [G.E. Hinton, S. Osindero, Y.W. Teh, A fast learning algorithm for deep belief nets, *Neural Comput.* 18 (2006) 1527–1554. <https://doi.org/10.1162/neco.2006.18.7.1527>.
 41. G.E. Hinton, R.R. Salakhutdinov, Reducing the dimensionality of data with neural networks, *Science* (80). 313 (2006) 504–507. <https://doi.org/10.1126/science.1127647>.
 42. J. Alphonsa, B.A. Padsala, B.J. Chauhan, G. Jhala, P.A. Rayjada, N. Chauhan, S.N. Soman, P.M. Raole, Plasma nitriding on welded joints of AISI 304 stainless steel, *Surf. Coatings Technol.* (2013). <https://doi.org/10.1016/j.surfcoat.2012.05.113>.
 43. J.C. Díaz-Guillén, G. Vargas-Gutiérrez, E.E. Granda-Gutiérrez, J.S. Zamarripa-Piña, S.I. Pérez-Aguilar, J. Candelas-Ramírez, L. Álvarez-Contreras, Surface Properties of Fe4N Compounds Layer on AISI 4340 Steel Modified by Pulsed Plasma Nitriding, *J. Mater. Sci. Technol.* (2013). <https://doi.org/10.1016/j.jmst.2013.01.017>.
 44. M. Asgari, A. Barnoush, R. Johnsen, R. Hoel,

- Microstructural characterization of pulsed plasma nitrided 316L stainless steel, *Mater. Sci. Eng. A.* (2011). <https://doi.org/10.1016/j.msea.2011.09.055>.
45. E. Maleki, O. Unal, S.M. Seyedi Sahebari, K.R. Kashyzadeh, A Novel Approach for Analyzing the Effects of Almen Intensity on the Residual Stress and Hardness of Shot-Peened (TiB + TiC)/Ti-6Al-4V Composite: Deep Learning, *Materials (Basel)*. 16 (2023) 4693. <https://doi.org/10.3390/ma16134693>
-